



Article

SWIPT-Assisted Energy Efficiency Optimization in 5G/B5G Cooperative IoT Network

Maliha Amjad ¹, Omer Chughtai ¹ , Muhammad Naeem ¹ and Waleed Ejaz ^{2,*} 

¹ Department of Electrical & Computer Engineering, Wah Campus, COMSATS University Islamabad, Wah Cantonment 47040, Pakistan; malihaamjad@ciitwah.edu.pk (M.A.); omer@ciitwah.edu.pk (O.C.); mnaeem@ciitwah.edu.pk (M.N.)

² Department of Electrical Engineering, Lakehead University, Barrie, ON L4M 3X9, Canada

* Correspondence: waleed.ejaz@ieee.org

Abstract: Resource use in point-to-point and point-to-multipoint communication emerges with the tremendous growth in wireless communication technologies. One of the technologies is wireless power transfer which may be used to provide sufficient resources for energy-constrained networks. With the implication of cooperative communication in 5G/B5G and the Internet of Things (IoT), simultaneous wireless information and power transfer (SWIPT)-assisted energy efficiency and appropriate resource use become challenging tasks. In this paper, multiple IoT-enabled devices are deployed to cooperate with the source node through intermediate/relay nodes powered by radio-frequency (RF) energy. The relay forwards the desired information generated by the source node to the IoT devices with the fusion of decode/amplify processes and charges itself at the same time through energy harvesting technology. In this regard, a problem with throughput, energy efficiency, and joint throughput with user admission maximization is formulated while assuring the useful, practical network constraints, which contemplate the upper/lower bounds of power transmitted by the source node, channel condition, and energy harvesting. The formulated problem is a mixed-integer non-linear problem (MINLP). To solve the formulated problem, the rate of individual IoT-enabled devices (b/s), number of selected IoT devices, and the sum-rate maximization are prosecuted for non-cooperation, cooperation with diversity, and cooperation without diversity. Moreover, a comparison of the outer approximation algorithm (OAA) and mesh adaptive direct search algorithm (MADS) for non-linear optimization with the exhaustive search algorithm is provided. The results with reference to the complexity of the algorithms have also been evaluated which show that 4.68×10^{-10} OAA and 7.81×10^{-11} MADS as a percent of ESA, respectively. Numerous simulations are carried out to exhibit the usefulness of the analysis to achieve the convergence to ϵ -optimal solution.

Keywords: 5G/B5G; cooperative communication; energy efficiency; energy harvesting; Internet of Things (IoT); optimization; resource management



Citation: Amjad, M.; Chughtai, O.; Naeem, M.; Ejaz, W. SWIPT-Assisted Energy Efficiency Optimization in 5G/B5G Cooperative IoT Network. *Energies* **2021**, *14*, 2515. <https://doi.org/10.3390/en14092515>

Academic Editors: Michael Alexandros Kourtis and Sangheon Pack

Received: 10 March 2021

Accepted: 21 April 2021

Published: 27 April 2021

Publisher's Note: MDPI stays neutral with regard to jurisdictional claims in published maps and institutional affiliations.



Copyright: © 2021 by the authors. Licensee MDPI, Basel, Switzerland. This article is an open access article distributed under the terms and conditions of the Creative Commons Attribution (CC BY) license (<https://creativecommons.org/licenses/by/4.0/>).

1. Introduction

The Internet of Things (IoT) is one of the growing fields comprised of devices that are capable of performing communication through wireless means with other integrated technologies via the Internet. IoT-enabled devices are deployed to execute different tasks as per the requirements of the applications, such as environment monitoring, smart homes and hospitals, remote access control and monitoring, etc. In addition, the nodes/devices deployed in an IoT-network are typically low-powered with other constraints such as limited buffer and energy capacity. Considering this fact, it is useful to charge a wireless network through energy harvesting technologies. There are several sources to harvest a particular device with the required energy. One of the sources is through the solar panel; however, another relatively inexpensive energy source is through the wind. Furthermore, wireless power transfer is another potential energy harvesting source. Such transfer of energy is fulfilled through the radio frequency signals. One must understand that

the traditional source of electricity is different from the energy harvesting mechanisms. Even though energy harvesting through radio frequency (RF) signals is a significant advancement, resource allocation for energy harvesting leads to more significant challenges, especially for an IoT-based network.

In an IoT-based network, the nodes/devices need to cooperate to use the network resources efficiently. To achieve better network efficiency, the network requires to support cooperative communication. In cooperative communication, intermediate or relays nodes are deployed to assist the source and the intended destination. Using the concept of cooperative communication in an IoT network can lead to efficient and fair resource use. However, to achieve the desired efficiency and fairness for resource allocation, the devices in an IoT-enabled network are assumed to be equipped with sensors, controllers, wireless transceivers, and energy sources. They are required to support communication through the Internet. In a typical IoT network, these devices that are deployed either deterministically or randomly can monitor several parameters such as humidity, pressure, temperature, etc., from the environment. However, these purely depend on the applications. In a practical IoT-network, in order to cover a large geographical area, a huge number of heterogeneous IoT-enabled devices are deployed. Each device communicates autonomously and cooperatively transmits its data to a central location such as a sink node for processing or storage. Such networks endure many challenges, such as energy-efficient, cooperative communication between nodes, along with the network's scalability issue.

In the practical deployment of an IoT network with 5G support, the major challenge is the sufficient energy supply to fulfill the QoS requirements of the network. As the IoT-enabled devices are very small and usually battery-powered, they have a limited power supply. These nodes are mostly deployed at remote or strategic locations where battery replacement is not humanly possible. When data processing and continuous transmission by IoT-enabled devices take place, energy depleted very fast in such an environment. To sustain this, the challenge is to improve energy efficiency and maintain the long-term and self-sustainable operation of the network. Numerous methods and procedures have been proposed in the literature to design and develop lightweight communication protocols [1–3], application-layer communication protocol [4], and the design of smart transceivers as discussed in [5]. To overcome the issues mentioned above and produce a perpetual operation of IoT-enabled devices, energy harvesting is contemplated to guarantee a self-powered device. Looking into the sensors used for military purposes, it gets to be more vital that the sensors embedded on the IoT devices ought to have the capability to function autonomously for a longer duration. Thus, a clear market-need exists that either allows the wireless device to operate for a longer duration away from the centralized power source or increases the amount of power supplied to the wireless device. As already discussed that there are several sources to harvest the energy, such as through renewable sources such as geothermal, wind, and solar as studied in [6], where the experimental study has been carried out and concluded that the sources, relays, and IoT-enabled devices require natural energy harvesting solutions and cannot be used in a network where the Quality-of-Service (QoS) requirement is a significant concern. Such issue has also been discussed in [7], where it has been highlighted that the IoT-enabled devices with power and resource constraints, the conventional sources for energy harvesting are not compatible.

Energy harvesting through a microwave signal and/or through RF are the most popular types. There are several advantages of using energy harvesting through the Radio Frequency; these are inexpensive, always available, and small form factor implementation of the energy harvester. An essential characteristic of Radio Frequency-Energy Harvester (RF-EH) is that RF signal permits simultaneous wireless information and power transfer (SWIPT). Additionally, it has been discussed in [8] that under a nonlinear EH model, a minimal required transmit power is much lower than used in linear EH model. Vershney et al. [9] conceived the idea and explored the characteristic of RF signal, which allows SWIPT. It is a process in which the energy is derived from external sources by scavenging DC from propagating RF radiation generated by near-by electronic devices, i.e., cell

phones, transmitting stations, radio broadcast, digital radio broadcast GSM downlinks, mediumwave broadcast, and Wi-Fi access points. SWIPT has been used and applied in various networks. One of the prominent examples is the successful implication of SWIPT in several low-power cellular network scenarios discussed in [10–12].

A good amount of research and development is being carried out in the direction of using SWIPT. One of the promising solutions which are being explored through cooperative communication (CC). It is to be noted that CC is a very strong concept of communication to increase transmission, capacity and overcome battery life problems, especially the network performance. The CC uses intermediate nodes/relays in a specific way. A cooperative wireless network comprises relay nodes, which uses to transfer information between the source and destination. Normally, the idle users in the network are used to relay the information, which means their energy is consumed to serve the active user, results in a decrease in battery life. When energy harvesting (EH) is incorporated in a network's relays, the energy efficiency, reliability, power, and QoS of the network are improved. Commonly two relay strategies are used in cooperative communication. These are amplified and forward (AF) and decode and forward (DF). AF procedure tries to amplify and retransmits the received signal transmitted by the source node. In addition, a DF relay can decode and re-modulate the received signal; however, after the required processing, it retransmits the received signal to the destination. In the scenario where DF-EH relays are used, the energy harvesting and information decoding are not usually performed simultaneously [13,14]. The steps are performed separately using time-switching or power-splitting techniques because of the limitation of practical circuits. Energy harvesting and data processing at the same time are complicated options in electronics. In point-to-point and multi-hop networks, the intermediate relay nodes used to assist source and destination can be configured to support all types of communication modes such as simplex, half, or full-duplex.

Resource use in point-to-point and point-to-multipoint communication emerges with the tremendous growth in wireless communication technologies. One of the technologies is wireless power transfer which may be used to provide sufficient resources for energy-constrained networks. With the implication of cooperative communication in 5G/B5G and the IoT, simultaneous wireless information and power transfer (SWIPT)-assisted energy efficiency and appropriate resource use become challenging tasks. In this paper, multiple IoT-enabled devices are deployed to cooperate with the source node through intermediate/relay nodes powered by RF energy. The relay forwards the desired information generated by the source node to the IoT devices with the fusion of decode/amplify processes and charges itself at the same time through energy harvesting technology. In this regard, a problem with throughput, energy efficiency, and joint throughput with user admission maximization is formulated while assuring the useful, practical network constraints, which contemplate the upper/lower bounds of power transmitted by the source node, channel condition, and energy harvesting. The formulated problem is a mixed-integer non-linear problem (MINLP). To solve the formulated problem, the rate of individual IoT-enabled devices (b/s), number of selected IoT devices, and the sum-rate maximization are prosecuted for no-cooperation, cooperation with diversity, and cooperation without diversity. Moreover, a comparison of the outer approximation algorithm (OAA) and mesh adaptive direct search algorithm (MADS) for non-linear optimization with the exhaustive search algorithm is provided. The results with reference to the complexity of the algorithms have also been evaluated which show that 4.68×10^{-10} OAA and 7.81×10^{-11} MADS as a percent of ESA, respectively. Numerous simulations are carried out to exhibit the usefulness of the analysis to achieve the convergence to ϵ -optimal solution.

2. Literature Review

Substantial investigation efforts have been committed within the scope of efficient and fair resource management for energy harvesting using cooperative communication. The following section discusses a few efforts in this domain. Table 1 provides some of the studies which have cooperatively used IoT and EH. The literature has been investigated

concerning numerous parameters and characteristics of the entities deployed in an IoT-based network along with the practical constraints of 5G and B5G, i.e., the single or a multi-relay network, the capability of energy harvester, the throughput of an individual IoT-user or overall throughput, energy efficiency, support of joint throughput and user maximization, QoS requirements for the modeling of a network, the defined optimization problem and the respective solution. The processes used in this work, such as AF and DF, are also used in [15]. However, this use is for the protocols used in continuous and discrete-time energy harvesting. A network model is considered with only a single power source and intermediate/relay nodes. It has been highlighted that energy harvesting can be applied to any transmission block in the aspect of continuous-time. On the other hand, the overall block in discrete time is used for information transfer in discrete-time energy harvesting.

Table 1. State of the art literature of resource management in IoT-Networks with 5G/B5G communication in energy harvesting cooperative networks; where Single relay (S), as well as Multiple relays (M), are considered, here, EH: Energy Harvesting, EE: Energy Efficiency, PA: Power Allocation, AC: Admission Control, QoS: Quality of Service.

Solution/Method	Relay		EH	EE	PA	AC	QoS	Multi-User	Optimization Type
	S	M							
Analytical approach [15]	✓		✓				✓		
Greedy algorithm [16]		✓			✓				
Heuristic [17]		✓		✓	✓				MINLP-C
Heuristic [18]			✓	✓	✓		✓		MINLP-NC
Heuristic [19]		✓	✓		✓			✓	MINLP-C
Analytical [20]		✓					✓	✓	
Heuristic [21]	✓		✓		✓				MINLP-C
Heuristic [22]	✓		✓		✓				MINLP-C
Analytical [23]	✓		✓						MINLP-C
Iterative subgradient descent method [24]	✓		✓		✓				Concave
Semidefinite relaxation & bisection techniques [25]		✓	✓		✓		✓	✓	
Greedy clustering algorithm [26]	✓		✓		✓				MINLP-C
Analytical [27]	✓		✓		✓			✓	
Interior-point method [28]		✓	✓						MINLP-C
Lagrange duality method [29]	✓		✓		✓			✓	MINLP-NC
Heuristic [30]	✓		✓		✓				MINLP
Asymptotic [31]			✓					✓	
Heuristic [32]		✓	✓						
Iterative heuristic algorithm [33]			✓	✓	✓			✓	MINLP
Greedy maximal scheduling algorithms [34]			✓		✓			✓	

Table 1. Cont.

Solution / Method	Relay		EH	EE	PA	AC	QoS	Multi-User	Optimization Type
	S	M							
Closed form expression with self sustaining novel protocol [35]	✓		✓						
Cooperative system with decode and forward approach [36]	✓		✓						Markov Decision Process
Convex form-based iterative algorithm [37]		✓	✓	✓	✓			✓	MINLP
ODS and AOP [38]	✓			✓	✓				Quasi Concave
CCCP-based iterative algorithm [39]	✓		✓	✓	✓				Quasi Concave
Iterative algorithm and Lagrange dual method [40]	✓		✓	✓					MINLP-C
OPA one time power allocation [41]		✓	✓	✓	✓		✓		Non-Convex
Pareto Optimality [42]							✓	✓	Game Theory
Hybrid resource management scheme [43]							✓	✓	Game Theory
Resource allocation Approach [44]				✓	✓				Non-Convex
ϵ -Optimal (This work)	✓	✓	✓	✓	✓	✓	✓	✓	MINLP

A greedy algorithm in a multi-relay network that considers the cooperative communication to achieve the sum-rate maximization and solve the power allocation is discussed in [16]. A mechanism that uses amplify and forward procedure to solve the power allocation and joint relay assignment is proposed in [17]. In addition, a heuristic mechanism has been adopted to achieve the desired solution based on the SWIPT cooperative network. Another problem that uses the power allocation for a non-convex optimization problem is considered in [18]. A heuristic algorithm is proposed to achieve a solution with the QoS constraints. Along with the heuristic algorithm, capacity maximization is achieved through power allocation to increase energy efficiency. Another heuristic approach that considers the convex optimization problem to model the power allocation and joint relay assignment is discussed in [19]. The relay selection procedures have also been proposed in the literature; one of the notice examples is discussed in [20], where a cognitive radio network has been considered with beacon-assisted dual hops. In [21], authors assumed a deterministic energy harvesting model to maximize the throughput using an energy harvesting source for the orthogonal relay channel.

A multi-carrier with a decode-and-forward procedure is discussed for a time-splitting-based relaying mechanism to achieve power allocation through a joint time-switching approach in [22]. Similarly, energy harvesting through a decode-and-forward procedure in order to investigate the PSR/TSR protocols for the maximum transmission rate in [23]. This work considers the convex optimization problem with the usability of a single relay network to achieve sum-rate maximization. Another approach discussed in [24] that considers a decode-and-forward procedure using half-duplex communication mode with the two-way transmission is investigated to achieve optimal power allocation. In addition, a subgradient descent algorithm has been used to achieve throughput maximization.

An approach that considers secure multicasting and SWIPT mechanism discussed in [25] with the implication of the decode-and-forward procedure through multiple eavesdroppers and receivers are investigated.

A SWIPT-based decode-and-forward procedure is investigated in [26], using a “harvest-then-use” approach to forward the desired information to the destination, and along with this, the joint-relay allocation has been proposed. Additionally, a greedy approach is adopted to decrease the implementation cost for antenna clustering. The antenna used to provide clustering is partitioned into two disjoint groups. One of the partitioned antennas is used for energy harvesting, and the other one is used for information decoding. A wireless energy harvesting protocol is proposed in [27], considering multiple primary users for an underlay cognitive relay network. Similarly, a SWIPT-based cooperative network with two-hop communication is investigated in [28] to implement a power splitting mode with the decode-and-forward procedure. Here, an interior-point methodology has been used for the relay assignment in a convex problem. Multiple source-destination pairs have been considered in a relay-assisted network with a hybrid mechanism. A constant supply is provided through the charge-then-forward protocol in [29]. The charge-then-forward protocols implemented on a relay node use frequency division multiple access to forward the desired information to the intended destination. Beyond that, it acts as an energy transmitter. Additionally, a procedure that has achieved the sum-rate maximization using the Lagrange duality method is investigated by optimizing the frequency, time, and power resources. Another joint optimization problem is investigated in [30], where transmit power and power splitting ratio is considered while interference as a constraint is considered to maximize the sum-rate. A multi-input and multi-output system with the maximization of sum-rate have been considered in [31], which has used the underlay spectrum sharing for energy harvesting. In [32], packet delivery ratio has been maximized in a cooperative network using a transmission scheduling technique with multiple terminals.

In [33], energy efficiency improvement is studied with the joint consideration of energy harvesting and self-backhaul procedures in cellular networks. A greedy scheduling algorithm for multi-task computation for offloading in a multi-user environment is considered in [34], for mobile edge computing. A solution that used energy harvesting to charge the primary user in order to solve the power and spectrum issues of a low-powered wireless network in [35]. The system uses the hostile environment for the deployment of the proposed work. In [36], an error rate minimization problem has been investigated for the cooperative network with the implication of decode-and-forward procedures along with the energy harvesting relay node. Additionally, the wireless energy transferring network and energy harvesting mechanisms are studied in [37]. The maximization of energy efficiency is carried out with the consideration of outage probability and energy causality constraints. A similar mechanism to maximize the energy efficiency by considering a tradeoff between the spectral efficiency and the energy efficiency is investigated in [38], with the implication of SE requirements. A work that considers the maximization of energy efficiency is studied in [39] with joint power allocation mechanism and power splitting ratio. Here, a two-way amplify-and-forward relay mechanism has been used with the SWIPT procedure.

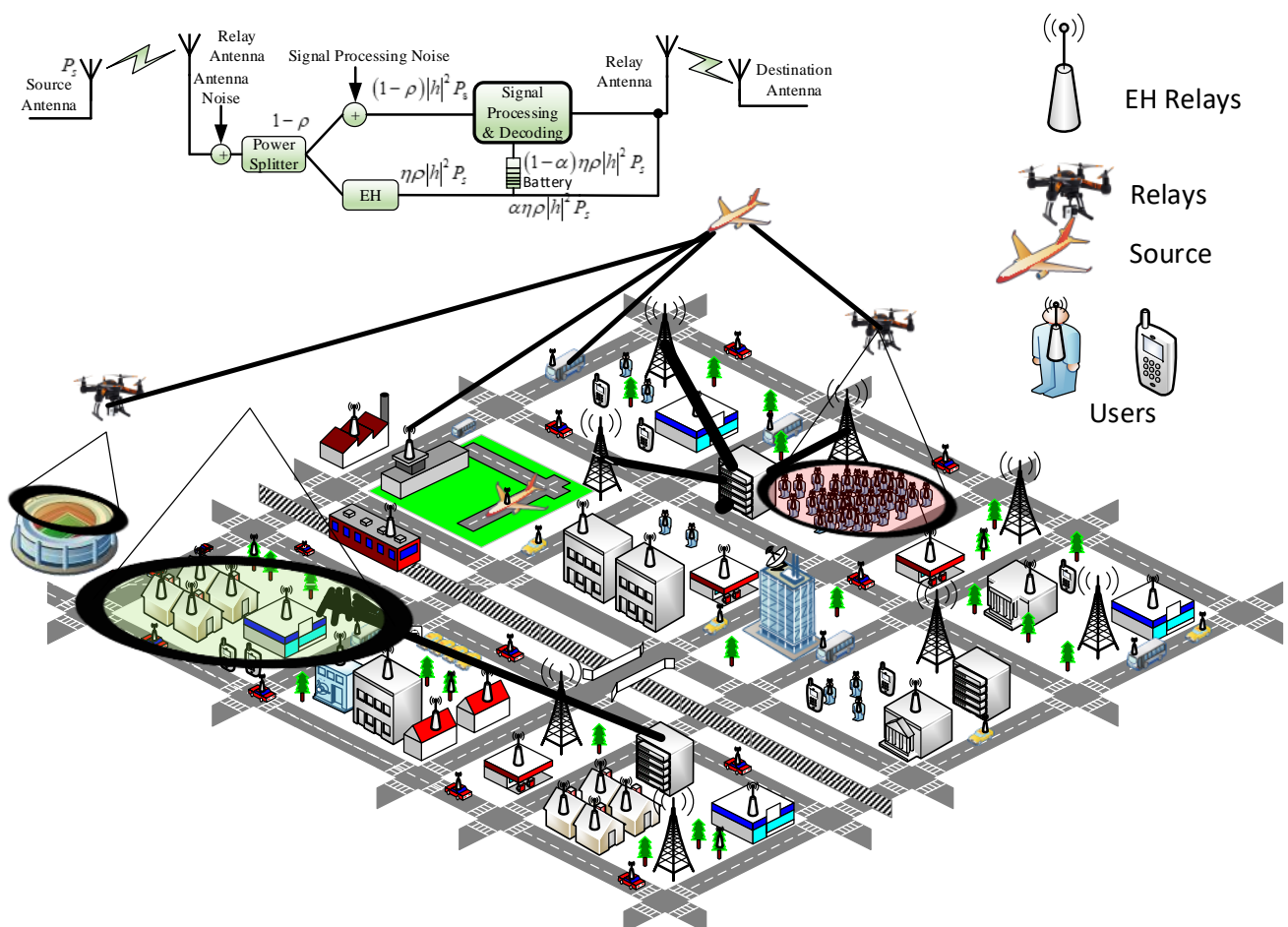
The total energy efficiency of all the deployed relay nodes and the sources is maximized in [40] by jointly optimizing the resource allocation by considering the number of sources and energy harvesting relay nodes, along with the mechanism used to select the appropriate relay. Additionally, the authors have proposed their work by using the concept of SWIPT. A mechanism that has investigated energy-efficient resource allocation in [41] by applying decode-and-forward along with the amplify-and-forward procedures to increase the energy efficiency at the intended destination with the usability of (SWIPT) cooperative networks. However, the authors have investigated the non-convex energy efficiency for the proposed work. Another work that has been studied to maximize its utility through the rate control and the power under the QoS constraints in [42]. To maximize the energy and bandwidth, which are considered scarce sources, has been proposed to understand

and the concepts of Game-theory approaches in [43]. However, it has been highlighted that the terminal life with wireless support is crucial to energy efficiency. In [44], the authors proposed a hybrid resource management procedure to maximize the energy efficiency in a 5G wireless network. This resource allocation mechanism satisfied the QoS requirements while achieving the desired objectives.

The summary of the related literature is given in Table 1. From the referenced table, it can be concluded that the existing literature for resource management has considered the energy harvesting mechanisms using a cooperative network. In contrast to this, in this work, throughput maximization, energy efficiency, and joint throughput, and user maximization are considered to evaluate the rate of individual IoT-enabled devices (b/s), the number of selected IoT devices, and the sum-rate maximization to the users. A detailed description of the model is presented in the following section.

3. System Model

Information sharing, connectivity, and power use are the keys to the smart city. The advanced communication technologies are no longer limited to provide Internet connectivity in the smart city. Presently, the smart city is visualized as a separate communication infrastructure with new technological concepts such as the IoT and 5G. Taking this into account, this work considers an IoT-enabled smart city scenario. To represent the flow of information and interconnection among different modules, a system model with a multi-relay architecture is considered as depicted in Figure 1. It incorporates two different solutions by considering scenarios with a single source communicating with multiple IoT-enabled devices through intermediate or relay nodes under 5G network constraints. Every node in the system is deployed to have different characteristics, such as the relay node is either used as an energy harvester or a UAV to forward the desired information to the intended destination. The relay node, which acts as an energy harvester, works with the principle of DF and assumes that it entirely relies on energy harvested from the RF signal generated by the source node. Similarly, IoT-enabled devices are used to collect data with reference to the application such as, on rainfall, temperature, wind speed, humidity, and traffic monitoring, etc. Analogously, the source node is used to render assistance as a SWIPT node.



It is to be noted that the information exchange among several entities in the system maneuver through cooperative communication. A source node is a transmitting node that begins RF Communication. The node that receives this information and is not the intended destination is the DF relay node i . It receives an RF signal from the source with power P_i ; however, the received signal might be a degraded distorted signal. In all circumstances, the relay node segregates the received RF signal into two distinct power components with a ratio $\rho_i \in [0, 1]$. One power component from the segregated components with power $\rho_i P_i$ is exploited as an energy harvester with $\eta \in [0, 1]$ efficiency. Concurrently, the second component with power $(1 - \rho_i) P_i$ is employed to trigger the step of signal processing and decoding. In conjunction with this, the first component used as an energy harvester yields the power signal as an output, $\eta \rho_i P_i$. Moreover, the harvested signal is further decomposed with a ratio α into two power factors. One power factor, which is $\alpha \eta \rho_i P_i$ is amalgamated with the decoded signal for retransmission, albeit, the second power factor, which is assorted as harvested power and represented as $(1 - \alpha) \eta \rho_i P_i$, is used as an energizer for the circuit used for signal processing and decoding.

Several notations were used in this work to represent the objective function and the constraints. K represents the total number of IoT-enabled users, and the corresponding number of relays is used to represent through R . The achievable transmit rate at the relay node is represented by C_k^1 . Similarly, C_k^2 is used for the user's achievable transmit rate. Additionally, for the binary indicator showing relay-user association, x_r^k notation is used. Furthermore, between relay r and user k , the source power splitting ratio, ρ_r is used. Likewise, P_s^k is used to represent the source power between source s and user k . Moreover, the maximum source power is used to represent through a notation as P_s^{max} , and R_k is used to represent a particular rate for user k . In addition, h_{sr} and h_{rk} are used to represent the channel gain between source s to relay r and between relay to user k , respectively. Each channel corresponds to a bandwidth which is represented as B . However, the variance of total noise from source s to relay r , s to k , and r to k , are represented through σ_{sr}^2 , σ_{sk}^2 , and σ_{rk}^2 , respectively. In this work, for energy harvesting efficiency, η is used, and the fraction of energy is harvested. Energy harvesting efficiency is represented by α .

Regarding the scenario depicted in Figure 1, three different communication cases are contemplated. Firstly, a non-cooperative (NC) communication case is considered. The source directly communicates with the destination – IoT-enabled devices, without using an intermediate node (relay). Secondly, cooperative communication without diversity is employed. The intermediate node participates as a relay node between the source and the destination. Lastly, a case of cooperative communication with diversity is applied, where the source communicates with the destination either through a direct link or a relay. Additionally, a cooperative multi-relay scenario bestows numerous benefits, such as an increase in the number of users, reliability, and the data rate. In the last two cases, where cooperation is an essential attribute, a source node transmits the RF signal, which the relay node might receive. However, the relay node decomposes the received signal into two components for each symbol duration T of the RF signal. In this decomposition, the DF procedure is carried out by the relay node to harvests the energy from the RF signal in the first half slot $\left(\frac{T}{2}\right)$ of duration T . Additionally, in the remaining second half slot of duration T , the retransmission is performed.

To mathematically formulate the expression for the decomposition of the RF Signal into two distinct slots in an IoT-enabled cooperative network, let us assume the number of users as K and the number of relays as R . The harvested energy during the first half slot $T/2$ from the received RF signal processed at r th relay for the k th user frequency band is given as [18]:

$$E_H^{rk} = \eta_r \rho_r P_s^k |h_{sr}|^2 \frac{T}{2}, \quad (1)$$

where η_r represents the efficiency for energy harvesting of a relay r , and the power splitting ratio at relay r symbolizes as ρ_r . Additionally, P_s^k is the transmit power from source s to k th user frequency band, and $|h_{sr}|$ is the complex channel gain between source s and relay r .

$$P_r^k = \frac{\alpha_r E_H^k}{T/2} = \frac{\alpha_r \eta_r \rho_r P_s^k |h_{sr}|^2 \frac{T}{2}}{T/2} = \alpha_r \eta_r \rho_r P_s^k |h_{sr}|^2. \quad (2)$$

As discussed earlier, the retransmission is carried out in the second half of the duration T so, α_r in Equation (2) is the portion of harvested energy transmitted in the second half ($T/2$). Now, considering the second case, which is the cooperative communication without diversity; the data rate of the wireless communication link from source to IoT-enabled k th user through a relay node with energy harvesting and DF capability is given as [15]:

$$R_{r,DF}^{WoDiv} = \frac{1}{2} \min \left\{ \log_2 \left(1 + Y_{DF}^1 \right), \log_2 \left(1 + Y_{DF}^2 \right) \right\}, \quad (3)$$

where the term $\frac{1}{2}$ exhibits that the transmission among the entities in the system is in half-duplex mode. Furthermore, σ_{sr}^2 and σ_{rk}^2 are the noise contributions in channel between source s to relay r , ($s \rightarrow r$) and relay to user k , ($r \rightarrow k$), respectively. Moreover in Equation (3) the first term, Y_{DF}^1 is the signal to noise ratio (SNR) that is defined as $\log_2 \left(1 + \frac{|(1-\rho_r)|h_{sr}|^2 P_s^k}{\sigma_{sr}^2} \right)$ and as a matter of fact, it shows the rate of channel between the source s and relay r , while on the contrary, the second term, Y_{DF}^2 is the SNR, which is defined as $\log_2 \left(1 + \frac{|h_{rk}|^2 P_r^k}{\sigma_{rk}^2} + \frac{|h_{sk}|^2 P_s^k}{\sigma_{sk}^2} \right)$ in Equation (3), indicates the rate of channel between relay r and the IoT-enabled user k . In principle, each IoT-enabled user k can get a chance to transmit so in order to refrain from congestion, primarily the total transmission rate for user k is the minimum of two rates. However, considering the third case where cooperative communication is carried out with diversity; the effective data rate from source s to user k , by consolidating the maximum ratio is given as:

$$R_{DF} = \frac{1}{2} \log_2 \left(1 + \frac{|h_{sk}|^2 P_s^k}{\sigma_{sr}^2} \right) + R_{r,DF}^{WoDiv}. \quad (4)$$

In energy harvesting mode, from now onward, P_r^k ; will be referred as the source power, this is because P_r^k is the function of source power that is $P_r^k(\rho, P_r^k)$, here, it is replaced by decision variable. Substituting the value of P_r^k from Equation (2) to (3), the rate in Equation (4) turn out to be:

$$R_{r,DF}^{WoDiv} = \min \frac{1}{2} \left\{ \log_2 \left(1 + \frac{(1-\rho_r)|h_{sr}|^2 P_s^k}{\sigma_{sr}^2} \right), \log_2 \left(1 + \frac{\rho_r \eta_r P_s^k \alpha_r |h_{sr}|^2 |h_{rk}|^2 + |h_{sk}|^2 P_s^k}{\sigma_{rk}^2 + \sigma_{sk}^2} \right) \right\}. \quad (5)$$

In contrast to DF, the data rate of communication link for cooperative communication without diversity from source s to k th IoT-enabled user through an energy harvesting relay node with amplify and AF capability is represented as:

$$R_{r,AF}^{WoDiv} = \frac{1}{2} \log_2 \left\{ 1 + \frac{|h_{sk}|^2 P_s^k}{\sigma_{sk}^2} + \frac{|h_{sr}|^2 |h_{rk}|^2 (1-\rho_r) P_s^k P_r^k}{1 + |h_{sr}|^2 (1-\rho_r) P_s^k + |h_{rk}|^2 P_r^k} \right\}. \quad (6)$$

In a situation with diversity and without diversity in the system as per the case mentioned above for amplify-and-forward, the respective rates regarding Equation (6) by substituting the value of P_r^k as $\alpha \eta \rho_r |h_{sr}|^2 P_s^k$, are represented as follows:

$$R_{r,AF}^{WoDiv} = \frac{1}{2} \log_2 \left\{ 1 + \frac{|h_{sr}|^4 |h_{rk}|^2 (1-\rho_r) P_s^k \alpha \eta \rho_r}{1 + |h_{sr}|^2 (1-\rho_r) P_s^k + \alpha \eta \rho_r |h_{sr}|^2 |h_{rk}|^2 P_s^k} \right\}, \quad (7)$$

$$R_{AF} = \frac{1}{2} \log_2 \left(1 + \frac{|h_{sk}|^2 P_s^k}{\sigma_{sk}^2} + \frac{|h_{sr}|^4 |h_{rk}|^2 (1-\rho_r) P_s^k \alpha \eta \rho_r}{1 + |h_{sr}|^2 (1-\rho_r) P_s^k + \alpha \eta \rho_r |h_{sr}|^2 |h_{rk}|^2 P_s^k} \right). \quad (8)$$

Considering the overall rate, the challenging task is the efficient IoT-enabled user to relay assignment by satisfying the QoS requirements of a cooperative IoT-based network with energy harvesting support, besides the best possible power allocation and splitting.

Problem Formulation

In this work, a mathematical model for cooperative communication under the condition of 5G through an IoT-enabled network with energy harvesting and resource management is formulated. Categorically, it incorporates a joint relay assignment for IoT-enabled devices with the consideration of source power and the contemplation of power splitting and the constraints of an IoT-enabled 5G network.

The description of a mathematical model with the joint user-relay assignment, source power, and splitting ratio selection problem formulated in this work is discussed in the following text as mathematically represented through **SWIPT5GOP1** and **SWIPT5GOP2**.

SWIPT5GOP1:

Decision Variables:

- X:** $K \times R$ Assignment matrix
- ρ :** $1 \times R$ Power splitting ratio vector
- P_s :** $1 \times K$ Source transmission power vector
- y :** $1 \times K$ Source transmission power vector

Objective Functions:

- OBJ1 :** $\max \{f_{\Gamma}^T(\mathbf{X}, \boldsymbol{\rho}, \mathbf{P}_s, \mathbf{y}) \mid \Gamma \in \{DF, AF\}\}$
- OBJ2 :** $\max \{f_{\Gamma}^{EE}(\mathbf{X}, \boldsymbol{\rho}, \mathbf{P}_s, \mathbf{y}) \mid \Gamma \in \{DF, AF\}\}$
- OBJ3 :** $\max \{f_{\Gamma}^{EE}(\mathbf{X}, \boldsymbol{\rho}, \mathbf{P}_s, \mathbf{y}); f_{\Gamma}^U(\mathbf{y}) \mid \Gamma \in \{DF, AF\}\}$

Constraints:

$$C1 : R_{\Gamma}(\mathbf{X}, \boldsymbol{\rho}, \mathbf{P}_s, \mathbf{y}) \geq y_k R_k^{min}, \forall k$$

QoS Constraint

Power constraints $\left\{ \begin{array}{l} C2 : \sum_{k=1}^K P_s^k \leq P_s^{max} \\ C3 : P_s^k \leq y_k P_s^{max}, \forall r, k \end{array} \right.$

Assignment constraints $\left\{ \begin{array}{l} C4 : \sum_{r=1}^R x_r^k \leq 1, \forall k \\ C5 : \sum_{k=1}^K x_r^k \leq 1, \forall r \\ C6 : x_r^k \leq y_k, \forall r, k \end{array} \right.$

$$C7 : \rho_r \leq \sum_{k=1}^K x_r^k, \forall r, k$$

Power Splitting Ratio Constraint

$$C8 : \rho_r \in [0, 1], x_r^k \in \{0, 1\}, y_k \in \{0, 1\}, P_s^k \geq 0, \forall r, k$$

Box Constraints

$$f_{\Gamma}^{EE}(\mathbf{X}, \boldsymbol{\rho}, \mathbf{P}_s, \mathbf{y}) = \frac{\sum_{k=1}^K \left(\frac{1}{2} \log_2 \left(1 + \frac{|h_{sk}|^2 P_s^k}{\sigma_{sr}^2} \right) \right) + \sum_{r=1}^R C_r^{WoDiv}}{P_c + \sum_{k=1}^K P_s^k} \tag{9}$$

$$f_{\Gamma}^T(\mathbf{X}, \boldsymbol{\rho}, \mathbf{P}_s, \mathbf{y}) = \sum_{k=1}^K \left(\frac{1}{2} \log_2 \left(1 + \frac{|h_{sk}|^2 P_s^k}{\sigma_{sr}^2} \right) \right) + \sum_{r=1}^R C_r^{WoDiv} \tag{10}$$

$$f_{\Gamma}^U(\mathbf{y}) = \frac{\sum_{k=1}^K y_k}{K} \tag{11}$$

For the relay with decode and forward capability, all the three objectives in **SWIPT5GOP1** represented as **OBJ1**, **OBJ2**, and **OBJ3** associated with a class of prob-

lems that are to maximize the minimum in nature, because of the expression given in Equation (5). The decision variables and the objectives represented in **SWIPT5GOP1** are reformulated with the augmentation of a new decision variable Ω_r^k as follows:

SWIPT5GOP2:

Decision Variables:

- X:** $K \times R$ Assignment matrix
 ρ : $1 \times R$ Power splitting ratio vector
 \mathbf{P}_s : $1 \times K$ Source transmission power vector
 \mathbf{y} : $1 \times K$ Source transmission power vector
 Ω : $K \times R$ Auxiliary variable

Objective Functions:

$$\text{OBJ1} : \max \{f_{\Gamma}^T(\mathbf{X}, \rho, \mathbf{P}_s, \mathbf{y}, \Omega) \mid \Gamma \in \{DF, AF\}\}$$

$$\text{OBJ2} : \max \{f_{\Gamma}^{EE}(\mathbf{X}, \rho, \mathbf{P}_s, \mathbf{y}, \Omega) \mid \Gamma \in \{DF, AF\}\}$$

$$\text{OBJ3} : \max \{f_{\Gamma}^{EE}(\mathbf{X}, \rho, \mathbf{P}_s, \mathbf{y}, \Omega); f_{\Gamma}^U(\mathbf{y}) \mid \Gamma \in \{DF, AF\}\}$$

Constraints:

C2 – C8 of **SWIPT5GOP1**:

$$\begin{aligned} \text{C1 of SWIPT5GOP1 reformulation} & \left\{ \begin{array}{l} \text{C9} : \frac{1}{2} \log_2 \left(1 + \frac{|h_{sk}|^2 P_s^k}{\sigma_{sr}^2} \right) + \frac{1}{2} \log_2 \left(1 + \frac{(1-\rho_r)|h_{sr}|^2 P_s^k}{\sigma_{sr}^2} \right) \geq y_k R_k, \forall k \\ \text{C10} : \frac{1}{2} \log_2 \left(1 + \frac{|h_{sk}|^2 P_s^k}{\sigma_{sr}^2} \right) + \frac{1}{2} \log_2 \left(1 + \frac{\rho_r \eta P_s^k \alpha |h_{sr}|^2 |h_{rk}|^2}{\sigma_{rk}^2} + \frac{|h_{sk}|^2 P_s^k}{\sigma_{sk}^2} \right) \geq y_k R_k, \forall k \end{array} \right. \\ \text{Objective functions SWIPT5GOP1 reformulation} & \left\{ \begin{array}{l} \text{C11} : \frac{1}{2} \log_2 \left(1 + \frac{(1-\rho_r)|h_{sr}|^2 P_s^k}{\sigma_{sr}^2} \right) \geq \Omega_r^k, \forall r, k \\ \text{C12} : \frac{1}{2} \log_2 \left(1 + \frac{\rho_r \eta P_s^k \alpha |h_{sr}|^2 |h_{rk}|^2}{\sigma_{rk}^2} + \frac{|h_{sk}|^2 P_s^k}{\sigma_{sk}^2} \right) \geq \Omega_r^k, \forall r, k \end{array} \right. \end{aligned}$$

The problem represented in **SWIPT5GOP2** is a mixed-integer non-linear problem (MINLP). It exhibits a primitive class of optimization problems with the variables associated as continuous and integer and the nonlinearities in the defined objective and/or the related constraints. Concerning MINLP, Γ in **SWIPT5GOP2** shows the type of relay protocol. It is to be noted that for both AF and DF processes of a relay node, it is used to maximize the performance metrics such as network throughput and energy efficiency while attaining the best unknown parameters $\mathbf{X}, \rho, \mathbf{P}_s, \mathbf{y}$.

With the consideration of cooperative communication with diversity, such as an admitted IoT-enabled user either connected directly to the source node or through the relay node. Consequently, the total energy efficiency and the received rate or throughput attained by the IoT-enabled end user are the sum of both the links: the direct communication link between the source and the IoT-enabled end-user and the indirect link between these two through an intermediate or a relay node. It is worth mentioning that 5G is the rationale for recognizing the full potential of IoT; thereby, the QoS requirements, which are considered the minimum achievable rate of 5G and the IoT-based network with practical constraints, are used to formulate the optimization problem.

For the cooperative communication using AF and DF techniques, the aforementioned objective functions represent the corresponding throughput and energy efficiency. Here, throughput is determined for the cooperative communication with diversity as expressed **SWIPT5GOP2**. To determine the energy-efficiency, this throughput needs to be divided with the total power, as expressed in Equation (9).

In the mathematical formulation, several constraints have been considered along with the desired objectives. These constraints provide restrictions on the optimization and characterize attainable plans. The constraints need to be satisfied. Otherwise, the results of the mathematical formulation based on the objectives through optimization are considered infeasible. Considering this fact, in this work, based on the **SWIPT5GOP1**; constraint

C1 reveals that an IoT-enabled user represented as k is only allowed to be the part of the system with the condition, i.e., (i.e., $y_k = '1'$) if it satisfies the QoS requirements, such constraint is referred as QoS constraint. Likewise, constraint C2 states that the sum of total transmit power of the source for all the IoT-enabled users must be upper bounded by a specific maximum value of the power as represented by P_s^{max} , such constraint is generally referred to as power budget constraint. Concerning constraint C3, it is stated that the power generated by the source can only be allocated to a specific admitted IoT-enabled user. Therefore, C2 and C3 are associated as power constraints. The constraints from C4 to C6 guarantee that only one user can communicate with a particular relay node. Similarly, only one relay is allowed to assist a specific IoT-enabled user. In other words, it can be stated as there must be a one-to-one relationship between the relays and the IoT-enabled users. A constraint for a relay node r represented as C7 ensures to perform energy harvesting with the power splitting ratio ρ_r , if it is a part of active communication between the source and the IoT-enabled user. This constraint is alluded to as a power splitting ratio constraint. Additionally, to represent the bounds of decision variables used in the communication, constraint C8 is used, which is associated as box constraint.

With the investigation and the exploration of the structure presented as an optimization problem, it is contemplated that the first portion of the defined objective function is concave, as its derivative function rigorously decreases on an interval. Analogously, the second portion of the objective function is the minimum of two BiConcave functions. However, the optimal solution must fulfill the following condition.

$$\log_2 \left(1 + \frac{(1 - \rho_r) |h_{sr}|^2 P_s^k}{\sigma_{sr}^2} \right) = \log_2 \left(1 + \frac{\rho_r \eta P_s^k \alpha |h_{sr}|^2 |h_{rk}|^2}{\sigma_{rk}^2} + \frac{|h_{sk}|^2 P_s^k}{\sigma_{sk}^2} \right), \quad (12)$$

or

$$\frac{(1 - \rho_r) |h_{sr}|^2}{\sigma_{sr}^2} = \frac{\rho_r \eta \alpha |h_{sr}|^2 |h_{rk}|^2}{\sigma_{rk}^2} + \frac{|h_{sk}|^2}{\sigma_{sk}^2}, \quad (13)$$

Solving Equation (14) gives:

$$\rho_r = \frac{\frac{|h_{sr}|^2}{\sigma_{sr}^2} - \frac{|h_{sk}|^2}{\sigma_{sk}^2}}{\frac{\eta \alpha |h_{sr}|^2 |h_{rk}|^2}{\sigma_{rk}^2} + \frac{|h_{sr}|^2}{\sigma_{sr}^2}}. \quad (14)$$

Taking into consideration the constraints C3 and C8 of **SWIPT5GOP1**, the optimal value of the power splitting factor will be:

$$\rho_r^* = \begin{cases} \max \left(\frac{\frac{|h_{sr}|^2}{\sigma_{sr}^2} - \frac{|h_{sk}|^2}{\sigma_{sk}^2}}{\frac{\eta \alpha |h_{sr}|^2 |h_{rk}|^2}{\sigma_{rk}^2} + \frac{|h_{sr}|^2}{\sigma_{sr}^2}}, 0 \right), & \text{if the } x_r^k = 1 \\ 0, & \text{otherwise.} \end{cases} \quad (15)$$

The constraint optimization problem mentioned in **SWIPT5GOP2** is also a mixed-integer non-linear programming problem, which is normally NP-Hard in nature. It is to be noted that when every problem in NP can be reduced in polynomial time to a decision problem, the problem is referred to as NP-Hard. However, the NP-Hard problem needs to be as hard as any NP-problem. The main issue while solving such kind of problems is their combinatorial nature of the domain of discrete variables $\mathbf{X} \in \{0, 1\}^{NK}$ and $\mathbf{y} \in \{0, 1\}^K$. Any choice of 0 or 1 for the discrete variables \mathbf{X} and \mathbf{y} results in a non-linear problem on the continuous variables ρ, P_s . To determine the best solution, it can be solved. To demonstrate the objective function represented in **SWIPT5GOP2**, a 3D plot of six cases of a channel is considered, as depicted in Figure 2. Here, a Rayleigh distribution is used to obtain the channel gain in each presented case. Here, the objective function is regular, uni-modal, in all the six cases; preferably, it can be stated as its local maxima are the global maxima.

Other approaches can also be applied to solve this problem, such as a brute-force approach. However, such kind of approaches is costly in terms of computation.

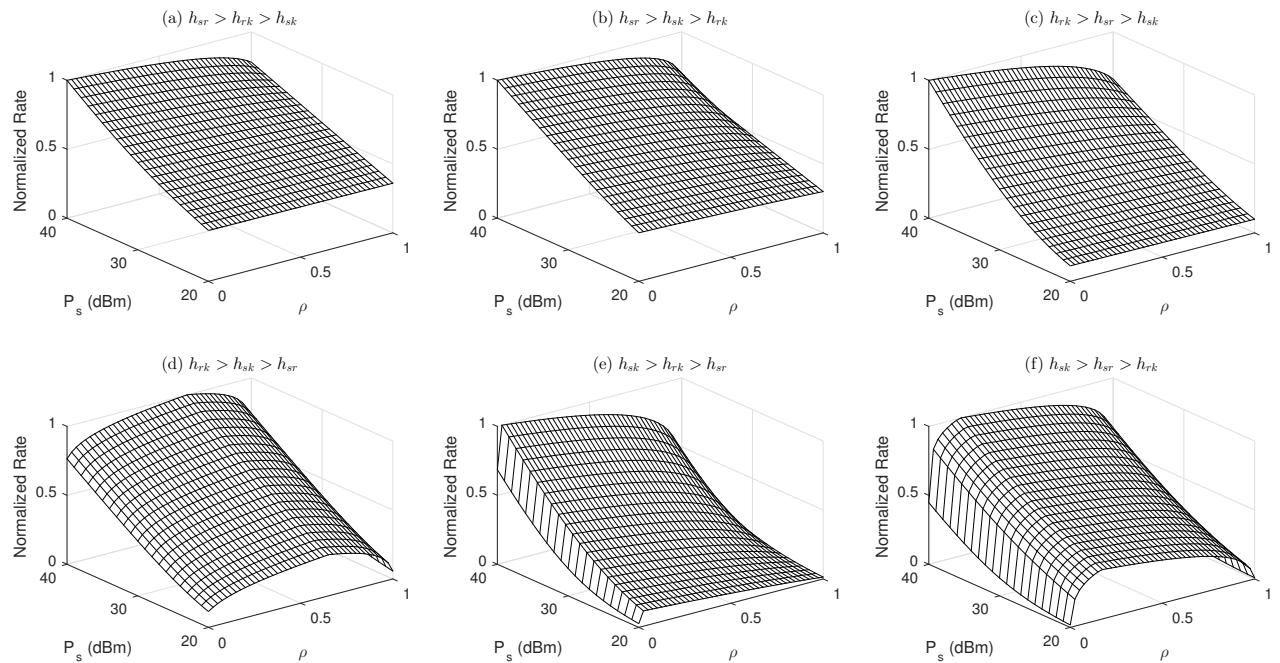


Figure 2. Objective function for different channel scenarios.

For each discrete realization of $\mathbf{X} \in \{0, 1\}^{NK}$ and $\mathbf{y} \in \{0, 1\}^K$ variables, the optimizer needs to solve one non-linear programming problem (NLP). Additionally, the search space for the computationally expensive approach, such as the brute force approach, is 2^{NK} , which pullulate exponentially with the increase in either the number of IoT-enabled devices or relays. Furthermore, such an exhaustive search enumerates all feasible discrete realization of x and y . However, enumerating all discrete realization is computationally very expensive. This is because each realization needs to solve one non-linear optimization problem. Moreover, even for a small search space, it is difficult to use an exhaustive search algorithm. Considering these facts and the structure of the optimization problem, low complexity algorithms are used, namely the OAA and MADS algorithm to solve the MINLP problem. Both of these algorithms are approximation algorithms. The OAA gives ϵ -optimal solution with guaranteed convergence. On the other hand, the NOMADs algorithm is also used to determine the ϵ -optimal solution; it uses the pattern search procedure by exploiting the mesh and polling search. The next section discusses the working principle of these two algorithms to solve the presented problem.

4. Proposed Approach to a Solution

The problem is challenging since it considers the coupling of a discrete integer with the continuous domain; however, considering the defined structure of the problem, it is contemplated that the problem is convex optimization for the variables maneuvering discrete realization with a continuous domain. In the light of the proposed outer approximation algorithm, which principally manipulates the given problem in **SWIPT5GOP2** into a series of mixed-integer problems and non-linear subproblems. Here, the series of mixed-integer problems is known as master problems [45,46]. Here, the non-linear contingent problem, which is the subproblem of a more inclusive problem **SWIPT5GOP2** that gives the upper bound for the actual MINLP problem is attained by using the fixed value of the binary integer decision variables $\mathbf{X} \in \{0, 1\}^{NK}$ and $\mathbf{y} \in \{0, 1\}^K$. Contrary to the non-linear

approximation of the main MINLP, the linear approximation is responsible for figuring out the lower bound of the problem. Both algorithms work iteratively to minimize the gap between the upper and the lower bounds to reduce the gap as much as possible so that the gap becomes less than the value of *epsilon*. The following subsections elaborate on the usability of MADS and OAA algorithms concerning the defined problem.

4.1. Nolinear Optimization Using MADS (NOMAD)

MADS algorithm is one of the suitable algorithms to find out the sub-optimal solution to a non-linear optimization problem. It is based on mesh and polling search mechanisms that work under the management of a pattern search algorithm, which determines the objective function through a local search in the vicinity of the current iterate [47]. Besides iterative procedure in MADS, it is also a frame-based and derivative-free algorithm. Using a MADS algorithm, a finite set of mesh points are determined throughout the solution search space. After a mesh search in the MADS algorithm, the polling step instigates the functionality that results in convergence. The procedure used in MADS is relatively considered as an iterative compression and/or expansion. It uses the predefined vicinity, locally based on its neighborhood, to search for the best possible option/location in different directions.

The procedure of MADS begins with the evaluation of the successive mesh points as represented with $NOMAD_s^1$ in the flowchart of MADS shown in Figure 3, using the defined objective function, which is then compared with the previous values determined through an objective function. If the comparison shows any escalation, then the subprocedure of MADS that is polling is initiated as shown through the step $NOMAD_s^2$ in the referenced Figure 3. Apart from that, with no escalation, the area of the mesh for a specific iteration k needs to be increased. The best location is pointed out through a generalized pattern search (GPS) procedure to place the stencil while executing the polling step, while there is a mismatch in the comparison. Generally, the stencil size is fixed in GPS. Furthermore, the mesh size used in the MADS algorithm is usually less than or equal to the stencil size, albeit, in GPS, the mesh size is equal to the stencil size.

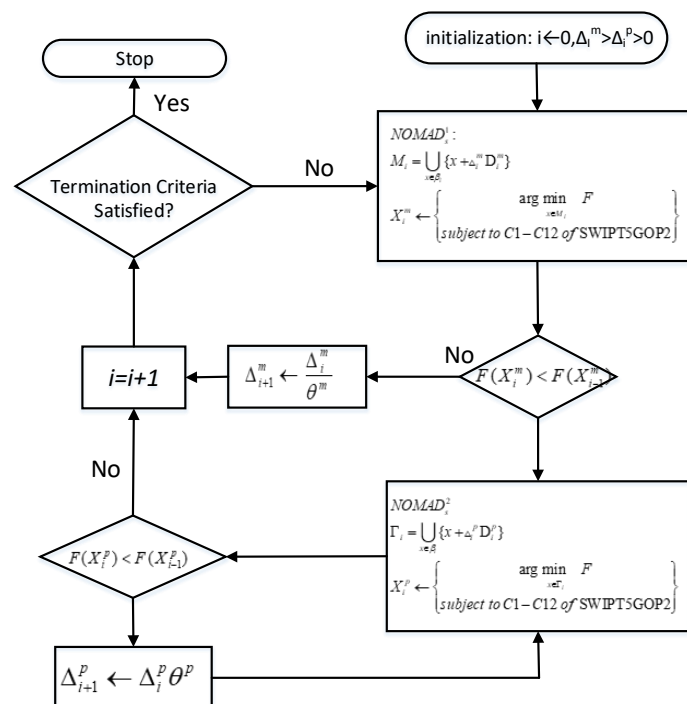


Figure 3. MADS flow chart.

The stencil, which has a poll stencil size, Δ_p^k , tries to see the solution for the convergence by searching around in four different directions (up, down, left, and right) in

its vicinity or neighborhood. In each location of the stencil, the objective function is computed. However, during this procedure, if the value of the objective function is less than the pre-determined points regarding the current stencil location, then the stencil pointer is relocated to the best point x_k among the four points within the vicinity for the next iteration $k + 1$. By considering this, the MADS algorithm can be able to investigate the larger search space. The above text explains the working principle of MADS in determining the better stencil location while increasing the mesh size; however, in the case with no further improvements, the corresponding stencil size decreased accordingly. Additionally, suppose the iteration could not find the better option. In that case, the grid size is decreased much quicker than the poll stencil size. In the literature, stencils with different sizes using MADS algorithm is discussed; a notice example is exhibited in [48]. The working principle regarding the steps involved in MADS is also illustrated through the flow chart as shown in Figure 3.

4.2. Outer Approximation Algorithm

Considering the NP-Complete class of joint resource allocation problem, it is implausible to figure out the optimal solution in polynomial time. As already discussed, the exhaustive search algorithm is computationally costly because it requires solving one non-linear optimization problem for each realization. In conjunction with this, to determine the optimal solution to a problem, this algorithm requires to iterate all one would require to enumerate all feasible sequences of IoT-enabled users in all given scenarios, which might exponentially increase the complexity of the problem. Considering these facts, one of the possible solutions which efficiently uses the structure of a problem and exploits the constraints as convex with the consideration of discrete variables as a known variable is generally referred to as the OAA. To describe the functionality of OAA for the defined objectives, assume the representation of the objective function as Γ^o and the constraint as Γ^c , respectively. For the realization of objective function $\mathbf{X} \in \{0, 1\}^{NK}$ and respective constraint $\mathbf{y} \in \{0, 1\}^K$ with regard to the discrete variables, it can be noted that these are differentiable and are compact, convex, and non-empty. Despite the given properties of the objective function and the relevant constraints, along with the consideration of a finite number of iterations [46,49], the proposed OAA algorithm converges the solution with ϵ value. The proposed OAA does not need to be only applicable to convex problems. Nonetheless, it is also applicable to non-convex problems, although it may be obstructed in determining the optimal local solution.

The defined objective function using OAA can be solved using a finite number of iterations by forming non-linear programming sub-problems. However, to proceed with the non-linear programming sub-problems using OAA, the discrete variables need to be considered as fixed, whereby the mixed-integer non-linear programming master problem (MILP-MP) requires to be flexible. Tagging along with these steps, a location is determined, which further produces the subspace whose dimension is less than that of the space surrounding a referenced point or location. Using OAA leads to generate one linearization against each objective function and the defined constraints at the end of these steps. The linearization for all the iterations is gathered in a MILP-MP. The detailed description of the proposed OAA is shown in Figure 4. Now, consider an original problem as shown in the flow chart of OAA through step 1, represented as OAA_s^1 . Suppose the representation of integer variables x and y for i th iteration are X^i and y^i , respectively. The values of these variables are assumed to be fixed in primal problem and are represented as:

$$\begin{aligned} \arg \min_{\rho, P_s} & -\Gamma^o(X^i, y^i, \rho, P_s) \\ \text{subject to:} & \Gamma^c(X^i, y^i, \rho, P_s) \leq 0. \end{aligned} \quad (16)$$

The solution determined from Step 2 in Figure 4 is used for the master problem, represented as OAA_s^2 , which yields the upper bound U with the known assignment variables X

and the selection variable y on the actual optimization problem. Likewise, to determine the lower bound and discrete variables for the next iteration, the original problem is solved as shown through Step 3 in the flow chart and represented as OAA_s^3 . The determined solution from the master problem is achieved by the primal problem using the OAA on the defined objective function $\Gamma^o(X^i, y^i, \rho, P_s)$:

$$\begin{aligned} & \min_{X,y} \quad \min_{\rho, P_s} \quad -\Gamma^o(X^i, y^i, \rho, P_s) \\ & \text{subject to:} \quad \Gamma^c(X^i, y^i, \rho, P_s) \leq 0. \end{aligned} \tag{17}$$

Furthermore, to subsequently linearize the problem using (X^i, y^i) is applied because of the defined objective function and constraint as convex. Therefore, the functions $\Gamma^o(X^i, y^i, \rho, P_s)$ and $\Gamma^c(X^i, y^i, \rho, P_s)$ using Step 4 are executed, represented as OAA_s^4 , and given as follows:

$$\begin{aligned} \Gamma^o(X, y, \rho, P_s) &\geq \Gamma^o(X^i, y^i, \rho, P_s) + \nabla \Gamma^o(X^i, y^i, \rho, P_s) \begin{pmatrix} X - X^i \\ Y - Y^i \end{pmatrix} \\ \Gamma^c(X, y, \rho, P_s) &\geq \Gamma^c(X^i, y^i, \rho, P_s) + \nabla \Gamma^c(X^i, y^i, \rho, P_s) \begin{pmatrix} X - X^i \\ Y - Y^i \end{pmatrix} \end{aligned} \tag{18}$$

The master problem represented in Equation (17), with the consideration of the above approximations, which is shown in in Equation (18), is formulated as follows:

$$\begin{aligned} & \min_{X,y} \quad \min_{\rho, P_s} \quad -\Gamma^o(X^i, y^i, \rho, P_s) + \nabla \Gamma^o(X^i, y^i, \rho, P_s) \begin{pmatrix} X - X^i \\ Y - Y^i \end{pmatrix} \\ & \text{subject to:} \quad \Gamma^c(X^i, y^i, \rho, P_s) + \nabla \Gamma^c(X^i, y^i, \rho, P_s) \begin{pmatrix} X - X^i \\ Y - Y^i \end{pmatrix} \leq 0. \end{aligned} \tag{19}$$

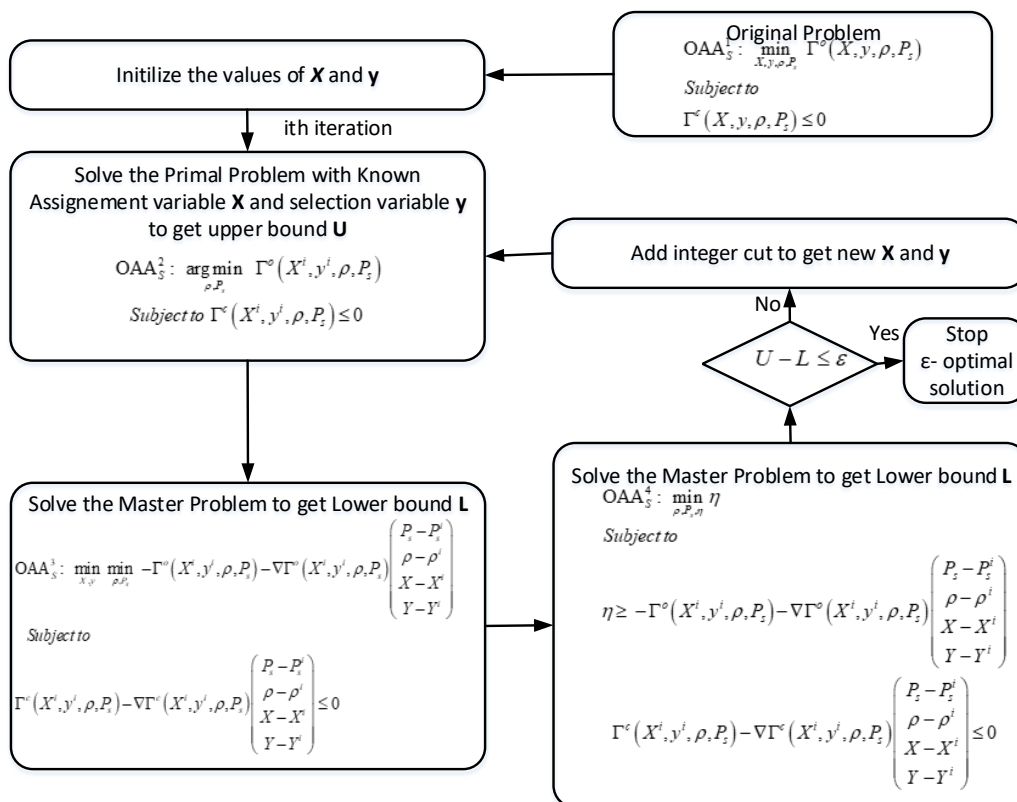


Figure 4. OAA flow chart.

It is to be noted that, to determine the lower bound, Step 4 is executed as represented through OAA_s^4 of the flow chart. These steps will execute. The algorithm is iterated until the difference between the upper bound and the lower bound becomes less than the value of ϵ . Here, the lower bound is determined from the master problem, and the upper bound is determined from the primal problem.

4.3. Complexity Analysis of Proposed NOMADS and OAA

Computation complexity is a phenomenon to determine the resources required to execute a given task. Regarding the algorithm, it is normally ascertained by the degree of flops, F or the number of floating points, which are the mathematical operation such as the arithmetic functions or the functions other than the binary integer operations. The following shows the list of several floating points used in this work:

1. Real arithmetic operations such as '+', '-', '×', and '/' measures one F for each instruction to be executed.
2. For operations in accordance with '+' or '-', two F are indispensable.
3. For complex operations in accordance with the '×' or '/', Four flops F are indispensable.
4. For the matrices with dimensions of $m \times n$ and $n \times o$, which are multiplied, $2mno$ flops F are required.
5. Among the mathematical operations, the logical operations require one flop F .

OAA: The first step that is OAA_s^1 requires one flop F for each corresponding instruction. However, to determine the convergence, a loop is required, and for that, it somehow takes $2|\mathcal{K}|^2$ flops. To determine the upper bound as represented through step OAA_s^2 , $4|\mathcal{K}|^2\beta$ flops are required. Similarly, for the lower bound, $2|\mathcal{K}|^2\beta$ flops are required. The total number of flops required in the OAA algorithm is:

$$Flops_{OAA} = 10 + 2|\mathcal{K}|^2 + 10|\mathcal{K}|^2\beta. \quad (20)$$

The following is the representation of the complexity in the form of Big- O notation:

$$Complexity_{OAA} \approx O(|\mathcal{K}|^2\beta). \quad (21)$$

In the above representations, $|\mathcal{K}|$ shows a pair of IoT-enabled users with D2D configurations. Here, β represents the number of constraints. The complexity of the OAA is the order of $|\mathcal{K}|^2\beta/\epsilon$ and is represented as $O(|\mathcal{K}|^2\beta/\epsilon)$. With the increase in the number of pairs of IoT-enabled users, the complexity of the problem increases by a square function of $|\mathcal{K}|$. The complexity might increase with the decrease in the value of ϵ , which is the difference between the upper and the lower bounds.

NOMAD: With the increase in the number of IoT-enabled users, the complexity that is $O(2^{2|\mathcal{K}|})$ increases exponentially for the Exhaustive search algorithm. However, with the consideration of MADS, it reduces because the convergence to a point referred to as ϵ -optimal represents a finite number of steps as also discussed in [50,51], which guaranteed by the MADS. The point that is to be noted here is the convergence in MADS, which is independent of the initial location/points for the sub-optimal solutions. However, the sub-optimal solution might have ϵ tolerance error from the solution, which is the global optimum. The big- O notation of MADS is $O(|\mathcal{K}|^2/\epsilon)$, where $|\mathcal{K}|$ represents the pair of D2D IoT-enabled users. The values tabulated in Table 2 show that MADS outperforms in terms of complexity as compared to ESA and OAA for twelve or greater values of the pair of IoT-enabled users having the configuration as D2D, with the consideration of β as 6 and ϵ as 0.001.

Table 2. Complexity Comparison (number of flops).

Parameters	ESA($2^{2 \mathcal{K} }$)	OAA ($\mathcal{K}^2\beta/\epsilon$)	OAA as Percent of ESA	MADS (\mathcal{K}^2/ϵ)	MADS as Percent of ESA
$ \mathcal{K} = 12$	1.68×10^7	8.64×10^6	51.5	1.44×10^6	8.6
$ \mathcal{K} = 16$	4.29×10^9	1.54×10^6	0.035	2.56×10^5	6×10^{-3}
$ \mathcal{K} = 20$	1.09×10^{12}	2.40×10^6	2.00×10^{-4}	4.00×10^5	3.00×10^{-5}
$ \mathcal{K} = 30$	1.152×10^{18}	5.40×10^6	4.68×10^{-10}	9.00×10^5	7.81×10^{-11}

5. Simulation Results

This section presents the proposed mechanisms’ simulation results, namely OAA and NOMAD, with different scenarios. Next-to-follow is the simulation results with the detailed discussion regarding the Energy efficiency and the joint utility of throughput, and user maximization is contemplated. Additionally, three main scenarios against NOMAD and OAA, which have been simulated using MATLAB (Mathworks, Natick, Massachusetts, USA), are listed as follows:

1. Without/No cooperation—NC
2. Cooperation with diversity— C_{Div}
3. Cooperation without diversity— C_{WoDiv}

In Figure 5, NOMAD and OAA were simulated with three different scenarios as listed above along with the implication of the defined objective functions. In these scenarios, the impact of several IoT devices on the individual rate (b/s) has been analyzed. The scenario depicted in Figure 5a,b considers 30 IoT devices K , where $K = \{4, 8, 12, \dots, 28\}$, and with 5 relay nodes R to analyze the individual rate achieved with the consideration of NOMAD and OAA by the considered one of the objective functions that are to maximize the throughput. The required rate is 1 Mbps, and the maximum power used in the given scenario is p^{max} , which is equal to 20 dbm. Regarding Figure 5a, it can be analyzed that with No Cooperation NC used in NOMAD, somehow, a smaller number of IoT-enabled devices are taken into account and hence leads to a decrease in the individual rate, which ultimately decreases the throughput (f_I^T). Contrary to this, OAA selects a smaller number of IoT devices than NOMAD under the same scenario and circumstances, such as the number of IoT devices K as 30 and the number of relay nodes R as 15. This is because OAA gives a non-optimal value when the problem is convex. The defined problem is not convex with the consideration of discrete realization.

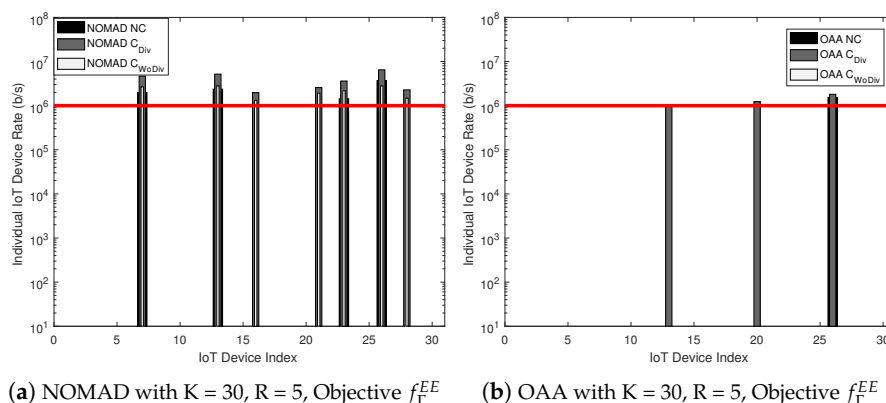


Figure 5. Cont.

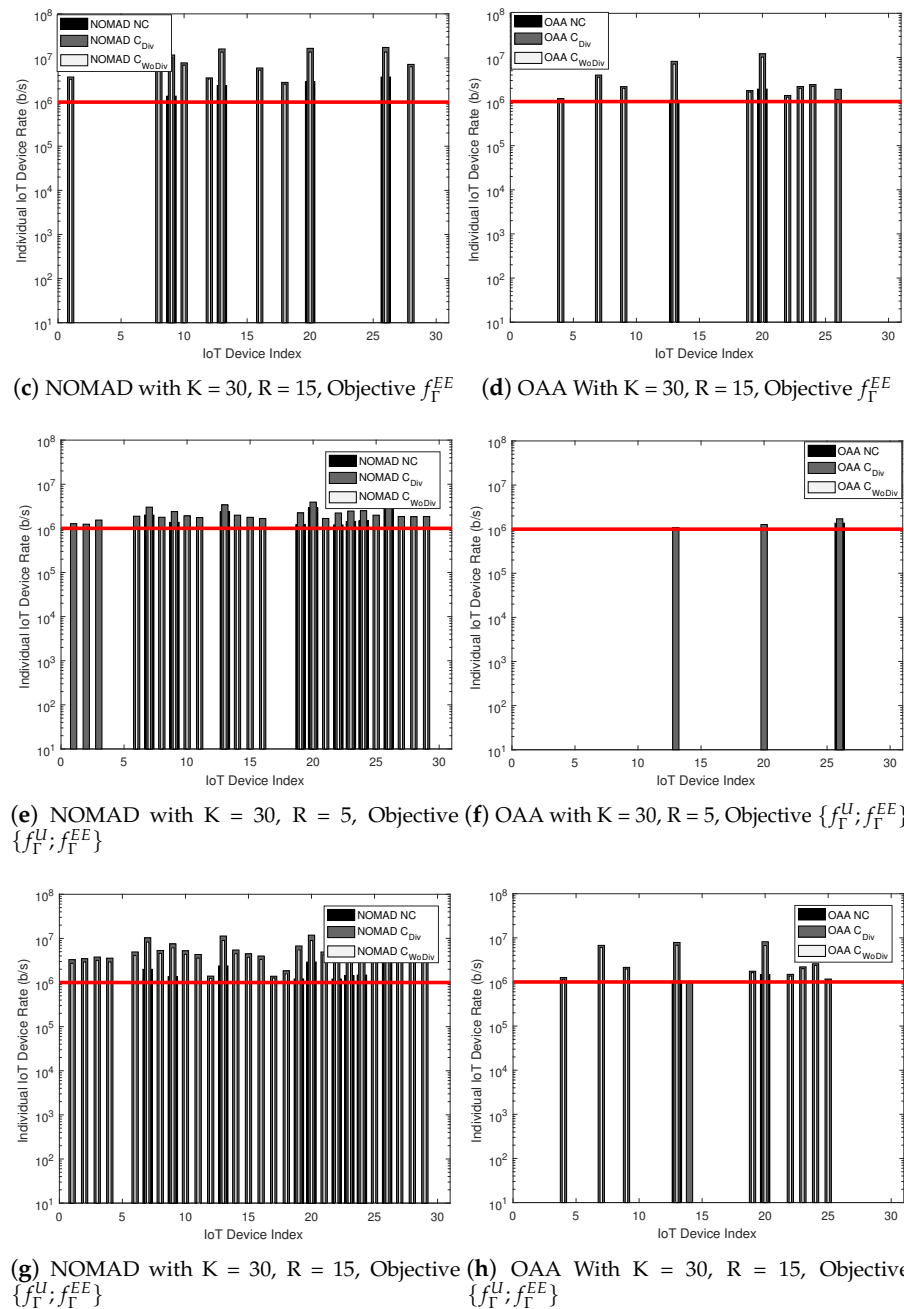
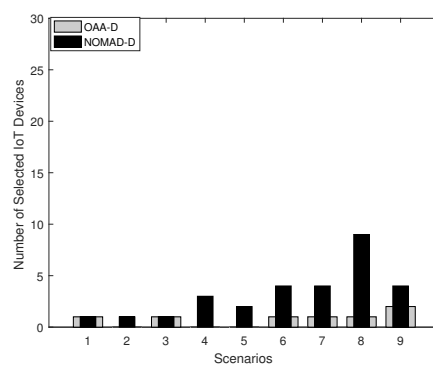


Figure 5. Rate of each IoT Device/Mobile Users for various parameters. Required rate 1 Mbps, $p_{max} = 20$ dbm.

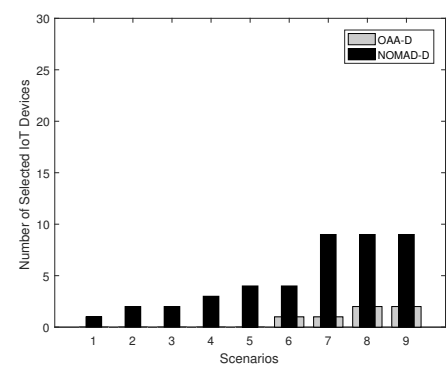
From the analysis, it is clear that the throughput achieved is always better in cooperation in all the cases in NOMAD. With cooperation, more relays have participated in the communication, and the system is able to satisfy the constraint used to provide QoS, such as data rate. In the same way, more IoT-enabled users are admitted, and eventually, the throughput increases. Besides that, the same trend is shown with cooperation, either with diversity or without diversity; however, with diversity, the rate increases because of the usability of multiple links. With this, the individual rate increases accordingly. Furthermore, as the number of IoT-enabled devices increases, the computational load ultimately increases; however, the computational complexity of OAA is higher than MADS. Moreover, MADS takes a finite number of steps to converge to ϵ -optimal solution compared to OAA. Likewise, with the consideration of objective function as energy efficiency (f_T^{EE}) as depicted from Figure 5c,d, the trend of taking into account the IoT-enabled devices

in NOMAD and OAA is somehow similar; however, the number of users are increased with the use of cooperation. This is because cooperation with diversity always gives a higher individual rate. It is to be noted that without joint utility, fewer users are selected; however at the same time, the individual rate becomes higher as compared to joint utility. In contrast to this, with joint user maximization and throughput utility $((f_T^T), (f_T^U))$, which is considered in Figure 5e–h, the individual rate increases; however, OAA shows a lesser number of individual rate. This is because as the number of IoT-enabled devices increases, the search space increases. Hence, the performance of OAA suffers compared to NOMADS. This is because of the computation complexity. With the joint utility and more relay nodes, the number of users accommodated in the communication using NOMAD and OAA increases. This is because the more number of relay nodes that accommodate more IoT-enabled users, the individual rate increases. Moreover, such an increase is because of the algorithm approach used in MADS, which is to apply the mesh search and then to poll search, as compared to OAA.

Figure 6 considers six different cases for the cooperation using OAA and NOMAD with diversity and without diversity are considered. It is to be noted that the communication channel used for communication is the same for all the cases. In these cases, the defined objectives with individual and joint utility have been implicated. The analysis is carried out for the K number of IoT-enabled devices, where K is considered 10, 20, and 30. Similarly, in the same manner, the number of relay nodes R increases as 5, 10, and 15. In the analysis, scenario indexes are used as $\{K,R\} : \{1,2,3,4,5,6,7,8,9\} = \{(10,5), (10,10), (10,15), (20,5), (20,10), (20,15), (30,5), (30,10), (30,15)\}$. This shows that scenario-1 considers K as 10 and R as 5, and similarly, scenario-9 considers K as 30 and R as 15. Overall the scenarios represent 9 pairs, which are used to analyze the number of selected IoT-devices with respect to the objective function using diversity and no-diversity. From the analysis, it is clear that with diversity, the number of selected IoT devices increases. It is also investigated that with a fewer number of users (IoT-enabled devices), OAA outperforms NOMAD; however, for the large scale problems, where the search space is large, which can accommodate more users, OAA degrades the performance.

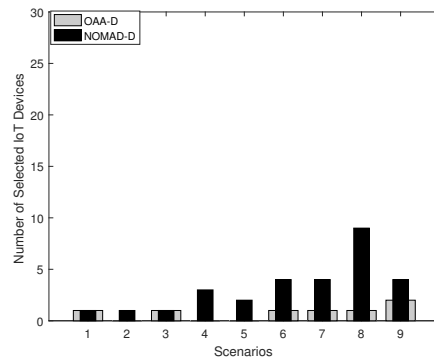


(a) Direct Transmission only f_T^{EE}

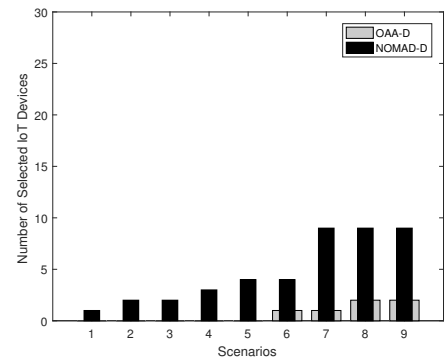


(b) Direct Transmission only, Objective $\{f_T^U, f_T^{EE}\}$

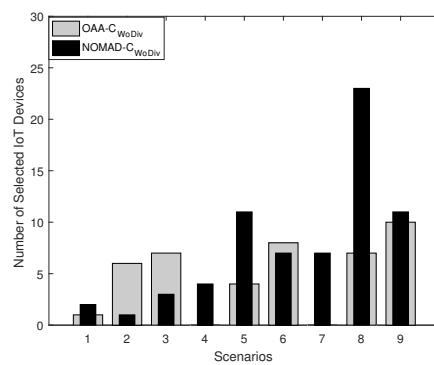
Figure 6. Cont.



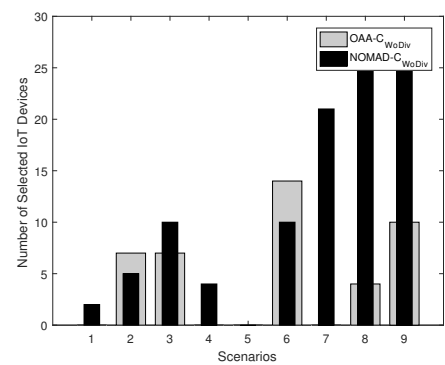
(c) Direct Transmission only f_T^{EE}



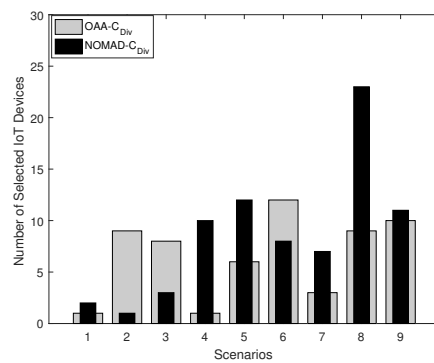
(d) Direct Transmission only, Objective $\{f_T^U, f_T^{EE}\}$



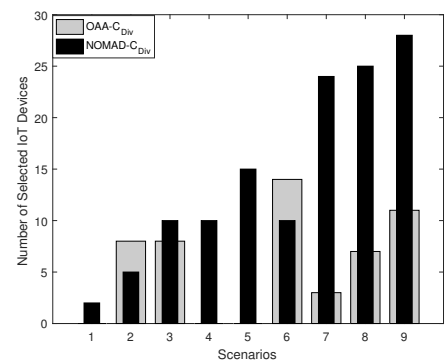
(e) Without Diversity, Objective f_T^{EE}



(f) Without Diversity, Objective $\{f_T^U, f_T^{EE}\}$



(g) With Diversity, Objective f_T^{EE}

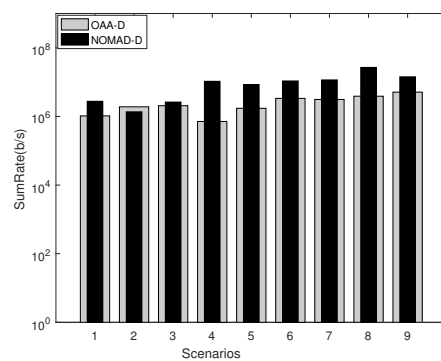


(h) With Diversity, Objective $\{f_T^U, f_T^{EE}\}$

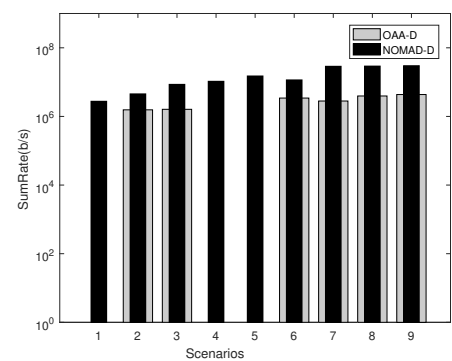
Figure 6. Number of Selected IoT Devices/Mobile Users for various parameters. Required rate 1 Mbps, $P^{max} = 20$ dbm. Scenarios are $\{K, R\}$: $\{1,2,3,4,5,6,7,8,9\} = \{(10,5),(10,10),(10,15),(20,5),(20,10),(20,15),(30,5),(30,10),(30,15)\}$.

In Figure 7, a comparison is carried out for sum-rate with respect to the number of IoT-enabled devices K and the number of relay nodes R . Here, K is used as 10, 20, and 30, whereas R is used as 5, 10, and 15. As in the previous case, in this analysis, scenario indexes are used as $\{K, R\} : \{1, 2, 3, 4, 5, 6, 7, 8, 9\} = \{(10, 5), (10, 10), (10, 15), (20, 5), (20, 10), (20, 15), (30, 5), (30, 10), (30, 15)\}$. This shows that scenario-1 considers K as 10 and R as 5, and similarly, scenario-9 considers K as 30 and R as 15. Overall the scenarios represent 9 pairs, which are used to analyze the number of selected IoT-devices for the objective function using diversity and no-diversity. In this scenario, the analysis is performed for the OAA and NOMAD using direct/no-cooperation, cooperation without diversity, and cooperation with diversity, as per the defined objective functions. It has been analyzed that with co-

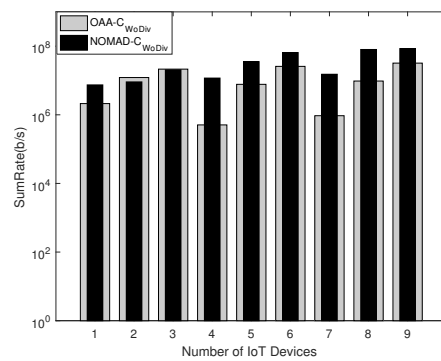
operation in all the cases, the achieved sum-rate shows a higher value. However, when the number of relay nodes increases, the system satisfies the QoS constraint, such as data rate. Additionally, with more relay nodes, more paths are formulated, which results in better communication. Furthermore, with more relay nodes, more IoT-enabled devices are accommodated in communication. Subsequently, the sum-rate is increased. From the analysis, it can be observed that the sum-rate becomes maximized with the consideration of diversity. However, with an increase in the number of relay nodes, the gap between cooperation and without cooperation has increased. This is because, with cooperation, more IoT-enabled devices can be accommodated/admitted. Therefore, it can be stated that with the increase in the number of relay nodes along with the diversity, the sum-rate can be increased. Conversely, the QoS requirements such as the data-rate could not be satisfied with fewer relay nodes considered in the system. So it can be concluded that with cooperative communication, the admitted user becomes higher if the diversity is used.



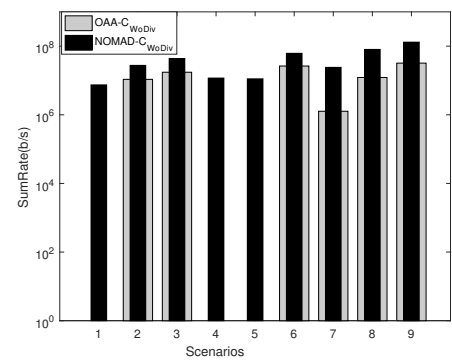
(a) Direct Transmission only f_{Γ}^{EE}



(b) Direct Transmission only, Objective $\{f_{\Gamma}^U, f_{\Gamma}^{EE}\}$



(c) Without Diversity, Objective f_{Γ}^{EE}



(d) Without Diversity, Objective $\{f_{\Gamma}^U, f_{\Gamma}^{EE}\}$

Figure 7. Cont.

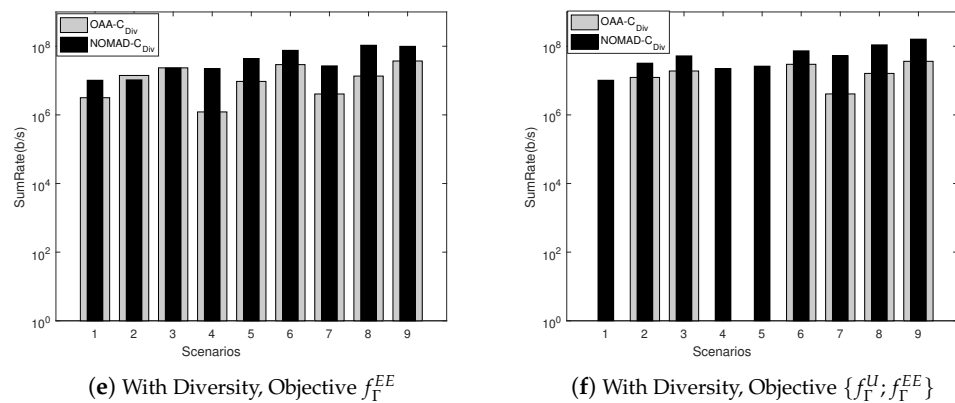


Figure 7. Sum Rate of IoT Devices/Mobile Users for various parameters. Required rate 1 Mbps, $p_{max} = 20$ dbm. Scenarios are $\{K, R\}$: $\{1,2,3,4,5,6,7,8,9\} = \{(10,5),(10,10),(10,15),(20,5),(20,10),(20,15),(30,5),(30,10),(30,15)\}$.

6. Conclusions

Cooperative communication using the Internet of Things (IoT) and 5G networks to supply energy using RF-signals to harvest the relay nodes have been brought up as a promising solution to increase the performance of the entire network. To exploit the IoT and 5G/B5G communication concepts' elegant features, an efficacious mechanism that provides the user-relay assignment is simulated for the proper splitting of transmitted power and efficient resource allocation. In this regard, a mathematical framework is proposed that implicates the amplify/decode and forward procedures in a cooperative IoT-network. In this framework, using SWIPT-assisted energy efficiency, the rate of individual IoT-enabled devices (b/s), the number of selected IoT devices, and the sum-rate maximization have been prosecuted with joint user-relay assignment through the transmit power with the consideration of the practical constraints of 5G/B5G communication. An OAA and NOMAD were simulated to achieve the optimal solution. The results showed that with the combination of cooperative communication with diversity, better IoT-enabled user admission control and the rate of individual IoT-enabled devices (b/s) and the sum-rate maximization are achieved.

Author Contributions: The initial concept of the problem and its mathematical modeling is performed by M.A. and M.N. Joint fruitful discussions with O.C. and W.E. helped to refine the formulation and its transformation to implementable form. Simulation and collection of useful results were jointly done by M.A., M.N. and O.C. Finally, O.C. and W.E. reviewed, checked, and corrected the final draft. All authors have read and agreed to the published version of the manuscript.

Conflicts of Interest: The authors declare no conflict of interest.

References

- Sheng, Z.; Zhu, C.; Leung, V. Surfing the Internet-of-Things: Lightweight Access and Control of Wireless Sensor Networks Using Industrial Low Power Protocols. *EAI Endorsed Trans. Indust. Netw. Intellig. Syst.* **2014**, *1*, e2. [[CrossRef](#)]
- Chu, Z.; Zhu, Z.; Johnston, M.; Le Goff, S.Y. Simultaneous wireless information power transfer for MISO secrecy channel. *IEEE Trans. Veh. Technol.* **2015**, *65*, 6913–6925. [[CrossRef](#)]
- Chu, Z.; Zhou, F.; Zhu, Z.; Hu, R.Q.; Xiao, P. Wireless powered sensor networks for Internet of Things: Maximum throughput and optimal power allocation. *IEEE Internet Things J.* **2017**, *5*, 310–321. [[CrossRef](#)]
- Bormann, C.; Castellani, A.P.; Shelby, Z. Coap: An application protocol for billions of tiny internet nodes. *IEEE Internet Comput.* **2012**, *16*, 62–67. [[CrossRef](#)]
- Jelicic, V.; Magno, M.; Brunelli, D.; Bilas, V.; Benini, L. Analytic Comparison of Wake-up Receivers for WSNs and Benefits over the Wake-on Radio Scheme. In *Proceedings of the 7th ACM Workshop on Performance Monitoring and Measurement of Heterogeneous Wireless and Wired Networks*; ACM: New York, NY, USA, 2012.

6. Panatik, K.Z.; Kamardin, K.; Shariff, S.A.; Yuhaniz, S.S.; Ahmad, N.A.; Yusop, O.M.; Ismail, S. Energy harvesting in wireless sensor networks: A survey. In Proceedings of the 2016 IEEE 3rd International Symposium on Telecommunication Technologies (ISTT), Kuala Lumpur, Malaysia, 28–30 November 2016; pp. 53–58. [[CrossRef](#)]
7. Joshi, R.; Zhu, J. Ambient energy harvester design for a wireless sensor network. In Proceedings of the 2015 IEEE International Conference on Electro/Information Technology (EIT), Dekalb, IL, USA, 21–23 May 2015; pp. 246–250.
8. Jiang, R.; Xiong, K.; Fan, P.; Zhang, Y.; Zhong, Z. Power minimization in SWIPT networks with coexisting power-splitting and time-switching users under nonlinear EH model. *IEEE Internet Things J.* **2019**, *6*, 8853–8869. [[CrossRef](#)]
9. Varshney, L. Transporting information and energy simultaneously. In Proceedings of the 2008 IEEE International Symposium on Information Theory, ISIT 2008, Toronto, ON, Canada, 6–11 July 2008; pp. 1612–1616. [[CrossRef](#)]
10. Lu, X.; Wang, P.; Niyato, D.; Kim, D.I.; Han, Z. Wireless Networks With RF Energy Harvesting: A Contemporary Survey. *IEEE Commun. Surv. Tutor.* **2015**, *17*, 757–789. [[CrossRef](#)]
11. Wing, D.; Ng, K.; Lo, E.S.; Schober, R. Wireless Information and Power Transfer : Energy Efficiency Optimization in OFDMA Systems. *IEEE Trans. Wirel. Commun.* **2013**, *12*, 6352–6370.
12. Zhang, R.; Ho, C.K. MIMO Broadcasting for Simultaneous Wireless Information and Power Transfer. *IEEE Trans. Wirel. Commun.* **2013**, *12*, 1989–2001. [[CrossRef](#)]
13. Liu, L.; Zhang, R.; Chua, K. Wireless Information Transfer with Opportunistic Energy Harvesting. *IEEE Trans. Wirel. Commun.* **2013**, *12*, 288–300. [[CrossRef](#)]
14. Zhou, X.; Zhang, R.; Ho, C.K. Wireless Information and Power Transfer: Architecture Design and Rate-Energy Tradeoff. *IEEE Trans. Commun.* **2013**, *61*, 4754–4767. [[CrossRef](#)]
15. Nasir, A.A.; Zhou, X.; Durrani, S.; Kennedy, R.A. Wireless-Powered Relays in Cooperative Communications: Time-Switching Relaying Protocols and Throughput Analysis. *IEEE Trans. Commun.* **2015**, *63*, 1607–1622. [[CrossRef](#)]
16. Bakanoglu, K.; Tomasin, S.; Erkip, E. Resource allocation in wireless networks with multiple relays. In Proceedings of the 2008 42nd Asilomar Conference on Signals, Systems and Computers, Pacific Grove, CA, USA, 26–29 October 2008; pp. 1501–1505.
17. Asiedu, D.K.P.; Mahama, S.; Jeon, S.; Lee, K. Joint Optimization of Multiple-Relay Amplify-and-Forward Systems Based on Simultaneous Wireless Information and Power Transfer. In Proceedings of the 2018 IEEE International Conference on Communications (ICC), Kansas City, MO, USA, 20–24 May 2018; pp. 1–6.
18. Guo, S.; Zhou, X. Energy-Efficient Design in RF Energy Harvesting Relay Networks. In Proceedings of the 2015 IEEE Global Communications Conference (GLOBECOM), San Diego, CA, USA, 6–10 December 2015; pp. 1–6.
19. Gupta, S.; Bose, R. Energy-aware relay selection and power allocation for multiple-user cooperative networks. In Proceedings of the 2016 IEEE Wireless Communications and Networking Conference, Doha, Qatar, 3–6 April 2016; pp. 1–7.
20. Hieu, T.; Duy, T.; Dung, L.; Choi, S. Performance Evaluation of Relay Selection Schemes in Beacon-Assisted Dual-Hop Cognitive Radio Wireless Sensor Networks under Impact of Hardware Noises. *Sensors* **2018**, *18*, 1843. [[CrossRef](#)]
21. Huang, C.; Zhang, R.; Cui, S. Throughput Maximization for the Gaussian Relay Channel with Energy Harvesting Constraints. *IEEE J. Sel. Areas Commun.* **2013**, *31*, 1469–1479. [[CrossRef](#)]
22. Huang, X.; Ansari, N. Optimal cooperative power allocation for energy-harvesting-enabled relay networks. *IEEE Trans. Veh. Technol.* **2016**, *65*, 2424–2434. [[CrossRef](#)]
23. Ju, M.; Kang, K.; Hwang, K.; Jeong, C. Maximum Transmission Rate of PSR/TSR Protocols in Wireless Energy Harvesting DF-Based Relay Networks. *IEEE J. Sel. Areas Commun.* **2015**, *33*, 2701–2717. [[CrossRef](#)]
24. Tutuncuoglu, K.; Varan, B.; Yener, A. Energy harvesting two-way half-duplex relay channel with decode-and-forward relaying: Optimum power policies. In Proceedings of the 2013 18th International Conference on Digital Signal Processing (DSP), Doha, Qatar, 3–6 April 2013; pp. 1–6.
25. Lee, J.H.; Sohn, I.; Kim, Y.H. Simultaneous Wireless Power Transfer and Secure Multicasting in Cooperative Decode-and-Forward Relay Networks. *Sensors* **2017**, *17*, 1128. [[CrossRef](#)]
26. Liu, Y. Joint Resource Allocation in SWIPT-Based Multiantenna Decode-and-Forward Relay Networks. *IEEE Trans. Veh. Technol.* **2017**, *66*, 9192–9200. [[CrossRef](#)]
27. Liu, Y.; Mousavifar, S.A.; Deng, Y.; Leung, C.; Elkashlan, M. Wireless Energy Harvesting in a Cognitive Relay Network. *IEEE Trans. Wirel. Commun.* **2016**, *15*, 2498–2508. [[CrossRef](#)]
28. Liu, Y. Wireless Information and Power Transfer for Multirelay-Assisted Cooperative Communication. *IEEE Commun. Lett.* **2016**, *20*, 784–787. [[CrossRef](#)]
29. Liu, M.; Liu, Y. Wireless Powered Relaying for Multiuser Transmission. In Proceedings of the 2017 IEEE Globecom Workshops (GC Wkshps), Singapore, 4–8 December 2017; pp. 1–6.
30. Lu, W.; Lin, Y.; Peng, H.; Nan, T.; Liu, X. Joint Resource Optimization for Cognitive Sensor Networks with SWIPT-Enabled Relay. *Sensors* **2017**, *17*, 2093. [[CrossRef](#)]
31. Al-Hraishawi, H.; Baduge, G.A.A. Wireless energy harvesting in cognitive massive MIMO systems with underlay spectrum sharing. *IEEE Wirel. Commun. Lett.* **2017**, *6*, 134–137. [[CrossRef](#)]
32. Ammar, A.; Reynolds, D. An adaptive scheduling scheme for cooperative energy harvesting networks. *J. Commun. Netw.* **2015**, *17*, 256–264. [[CrossRef](#)]
33. Chen, L.; Yu, F.R.; Ji, H.; Rong, B.; Li, X.; Leung, V.C.M. Green Full-Duplex Self-Backhaul and Energy Harvesting Small Cell Networks With Massive MIMO. *IEEE J. Sel. Areas Commun.* **2016**, *34*, 3709–3724. [[CrossRef](#)]

34. Chen, W.; Wang, D.; Li, K. Multi-user Multi-task Computation Offloading in Green Mobile Edge Cloud Computing. *IEEE Trans. Serv. Comput.* **2018**, *12*, 726–738. [[CrossRef](#)]
35. Jain, N.; Bohara, V.A. Energy Harvesting and Spectrum Sharing Protocol for Wireless Sensor Networks. *IEEE Wirel. Commun. Lett.* **2015**, *4*, 697–700. [[CrossRef](#)]
36. Ku, M.; Li, W.; Chen, Y.; Liu, K.J.R. On Energy Harvesting Gain and Diversity Analysis in Cooperative Communications. *IEEE J. Sel. Areas Commun.* **2015**, *33*, 2641–2657. [[CrossRef](#)]
37. Qi, N.; Xiao, M.; Tsiftsis, T.A.; Zhang, L.; Skoglund, M.; Zhang, H. Efficient Coded Cooperative Networks With Energy Harvesting and Transferring. *IEEE Trans. Wirel. Commun.* **2017**, *16*, 6335–6349. [[CrossRef](#)]
38. Huang, S.; Chen, H.; Cai, J.; Zhao, F. Energy efficiency and spectral-efficiency tradeoff in amplify-and-forward relay networks. *IEEE Trans. Veh. Technol.* **2013**, *62*, 4366–4378. [[CrossRef](#)]
39. Zhou, X.; Li, Q. Energy efficiency optimisation for SWIPT AF two-way relay networks. *Electron. Lett.* **2017**, *53*, 436–438. [[CrossRef](#)]
40. Zhao, N.; Chai, R.; Hu, Q.; Zhang, J.K. Energy efficiency optimization based joint relay selection and resource allocation for SWIPT relay networks. In Proceedings of the 2015 10th International Conference on Communications and Networking in China (ChinaCom), Shanghai, China, 15–17 August 2015; IEEE: Piscataway, NJ, USA, 2015; pp. 503–508.
41. Guo, S.; Zhou, X.; Zhou, X. Energy-efficient resource allocation in swipt cooperative wireless networks. *IEEE Syst. J.* **2020**, *14*, 4131–4142. [[CrossRef](#)]
42. Meshkati, F.; Poor, H.V.; Schwartz, S.C.; Balan, R.V. Energy-efficient resource allocation in wireless networks with quality-of-service constraints. *IEEE Trans. Commun.* **2009**, *57*, 3406–3414. [[CrossRef](#)]
43. Meshkati, F.; Poor, H.V.; Schwartz, S.C. Energy-efficient resource allocation in wireless networks. *IEEE Signal Process. Mag.* **2007**, *24*, 58–68. [[CrossRef](#)]
44. Nguyen, L.D. Resource allocation for energy efficiency in 5G wireless networks. *Eai Endorsed Trans. Ind. Netw. Intell. Syst.* **2018**, *5*. [[CrossRef](#)]
45. Fletcher, R.; Leyffer, S. Solving mixed integer nonlinear programs by outer approximation. *Math. Program.* **1994**, *66*, 327–349. [[CrossRef](#)]
46. Floudas, C.A. *Nonlinear and Mixed-Integer Optimization: Fundamentals and Applications*; Oxford University Press: Oxford, UK, 1995.
47. Isebor, O.; Durlinsky, L.; Echeverría Ciaurri, D. A derivative-free methodology with local and global search for the constrained joint optimization of well locations and controls. *Comput. Geosci.* **2014**, *18*, 463–482. [[CrossRef](#)]
48. Audet, C.; Dennis, J.E., Jr. Mesh adaptive direct search algorithms for constrained optimization. *SIAM J. Optim.* **2006**, *17*, 188–217. [[CrossRef](#)]
49. Duran, M.A.; Grossmann, I.E. An outer-approximation algorithm for a class of mixed-integer nonlinear programs. *Math. Program.* **1987**, *39*, 337. [[CrossRef](#)]
50. Konecny, J.; Richtárik, P. Simple Complexity Analysis of Direct Search. *CoRR* **2014**.
51. Abramson, M.A.; Audet, C.; Chrissis, J.W.; Walston, J.G. Mesh adaptive direct search algorithms for mixed variable optimization. *Optim. Lett.* **2009**, *3*, 35–47. [[CrossRef](#)]